JOURNAL OF CATALYSIS 115, 486–499 (1989)

Kinetics of NO Reduction by CO over Supported Rhodium Catalysts: Isotopic Cycling Experiments

BYONG K. CHO,*,[1] BRENT H. SHANKS,*,[2] AND JAMES E. BAILEY†

*Physical Chemistry Department, General Motors Research Laboratories, Warren, Michigan 48090-9055; and †Department of Chemical Engineering, California Institute of Technology, Pasadena, California 91125

Received May 24, 1988; revised September 6, 1988

The catalytic activity of Rh/Al_2O_3 and Rh/CeO_2 catalysts was investigated for the reduction of NO by CO under feed-composition cycling conditions as well as under steady feed conditions using a packed-bed reactor and an isotopic reactant, ^{13}CO. Results indicate that the formation of N_2O is an important *intermediate step* during the (CO + NO) reaction over Rh/Al_2O_3. The enhanced catalytic activity of Rh/CeO_2 compared with Rh/Al_2O_3 under cyclic operating conditions is discussed in light of the oxygen storage capacity of ceria support. The effect of asymmetric cycling is examined in view of the nature of the rate-controlling step which changes with temperature. On the basis of our observations an overall reaction scheme is proposed for the (CO + NO) reaction over Rh/Al_2O_3, in which N_2O is included as a reaction intermediate.

INTRODUCTION

Rhodium is an important ingredient of three-way catalysts used for the simultaneous conversion of hydrocarbons, carbon monoxide, and nitrogen oxides in automobile exhaust. It is widely recognized that Rh has superior low-temperature activity toward NO decomposition as well as toward CO oxidation compared with Pt and Pd (*1, 2*). Recently the importance of Rh in automobile emission control systems combined with its high price and scarcity has prompted extensive research efforts directed toward the reduction or replacement of the Rh requirement in three-way catalytic converters without adversely affecting the conversion performance (*3–6*). It is well known that entirely different exhaust environments are desirable for the reduction of NO and the oxidation of CO (or hydrocarbons); the oxidation of CO (or hydrocarbons) is favored by net oxidizing conditions, while the reduction of NO is favored by net reducing conditions. Thus, three-way catalysts are typically designed to operate near the stoichiometric point for simultaneous removal of all three pollutants (i.e., CO, hydrocarbons, and NO) by means of a feedback control mechanism (*2*). But normal oscillations in closed-loop emission control systems lead to the fluctuations of the exhaust composition to both the rich and the lean side of the stoichiometric set point. Consequently, it is of practical importance to understand the kinetic behavior of the (CO + NO) reaction under cycled feedstream conditions as well as under steady feedstream conditions.

As a result of recent extensive research efforts, the reaction mechanism for the reduction of NO by CO ($NO + CO \rightarrow \frac{1}{2}N_2 + CO_2$) on Rh catalysts appears reasonably well understood (e.g., *7–12*). However, there has been some controversy regarding N_2O formation during NO decomposition or (CO + NO) reaction on Rh catalysts, even though the importance of N_2O formation has been recognized on transition metals and their oxides (*13–15*). For example, Root *et al.* (*11, 16*) and Campbell and White (*9*) did not observe the N_2O formation on Rh(111) and polycrystalline Rh wire, respectively, while on Rh(s) − [6(111)

[1] To whom correspondence should be addressed.

[2] GMR Summer Student currently at Shell Development Company, Houston, Texas.

0021-9517/89 $3.00

× (100)] Castner and Somorjai (*17*) observed a significant amount of N_2O formation. On supported Rh catalysts the formation of N_2O during the (CO + NO) reaction has been seldom mentioned in the literature with the exception of recent studies by Hecker and Bell (*18, 19*) over Rh/SiO_2 catalysts. More recently Cho and Stock (*20*) also reported the formation of N_2O in their transient study of NO decomposition over Rh/Al_2O_3 and Rh/CeO_2 catalysts. During the course of this work we have consistently observed significant N_2O formation, and the importance of the N_2O formation step in the overall (CO + NO) reaction will be examined in detail in this paper.

A *transient* kinetic study by Cho and Stock (*20*) revealed that the activity of Rh/Al_2O_3 catalysts for NO decomposition is severely deteriorated by the accumulation of the surface oxygen derived from the NO decomposition. Cho and Stock (*20*) also demonstrated that the lifetime of Rh/Al_2O_3 catalysts for NO decomposition can be significantly extended by using an alternate support such as CeO_2 which has greater oxygen storage capacity than Al_2O_3. These findings suggest the possibility that cycled operation using CO as a reducing agent may regenerate the deactivated Rh catalysts by periodically removing the accumulated oxygen via reaction with adsorbed CO. In more traditional catalytic processes in the petroleum industry, the regeneration time for deactivated catalysts represents only a small fraction of the deactivation time, allowing in effect the decoupling of the regeneration process from the deactivation process. However, when the regeneration and deactivation times are of the same magnitude, the resulting close-coupling between the two processes makes the cycling period a critical parameter for the optimum performance of the cyclic operation (*21*). A recent investigation by Monroe and Leifermann (*22*) on the conversion efficiencies of warmed-up converters indicates that both the cycling period and the cycling amplitude have a major impact on the performance of catalytic converters. Thus, it is of practical interest to determine the relative rates of catalyst deactivation and regeneration under cyclic operating conditions.

In the work reported here, we first investigate the (CO + NO) reaction over Rh/Al_2O_3 catalysts under feed-composition cycling conditions as well as under steady feed conditions using an isotopic reactant ^{13}CO. The catalyst performance under cyclic operating conditions is compared with that under steady operating conditions. The importance of N_2O formation during the (CO + NO) reaction is also examined. Of particular interest are the relative rates of catalyst deactivation for NO decomposition and the subsequent catalyst regeneration by CO. We also demonstrate the beneficial effect of a ceria support on NO decomposition activity of Rh catalysts under cyclic operating conditions at 500°C.

TRANSIENT CYCLING AND STEADY-STATE EXPERIMENTS

Description of Experiments

Rhodium catalysts on two different supports were used in this study: Rh/Al_2O_3 and Rh/CeO_2. Both catalysts were prepared by impregnating the respective support (γ-Al_2O_3 or CeO_2) with $[(n\text{-}C_4H_9)_4N]_2[Rh(CO)Br_4]_2$ using a nonaqueous impregnation technique (*23*), so that a shallow noble metal band can be formed near the periphery of the support particles. Considering the difference between the densities of Al_2O_3 and CeO_2, the Rh loadings as weight percentages of the supports (see Table 1) were chosen so that the total amount of Rh contained in the same reactor volume is essentially the same. Following impregnation the catalysts were dried in air overnight at room temperature, heated slowly in flowing air up to 500°C, and then held at 500°C for 4 h. The noble metal dispersion was measured by CO chemisorption in the flow system assuming 1 : 1 stoichiometry between a surface metal atom and an adsorbed CO molecule for both Rh/Al_2O_3 and Rh/CeO_2 catalysts. The impregnation band-

TABLE 1

Catalysts and Reactor Characteristics

Supports				
Particle size		80–120 mesh (125–177 μm diameter)		
BET surface area		70 m^2/g (Al_2O_3)		
		0.3 m^2/g (CeO_2)		
Bulk density		2.046 g/cm^3 (Al_2O_3)		
		5.218 g/cm^3 (CeO_2)		
Catalysts				
	Rh loading (wt%)	Sample weight (g)	Impregnation depth (μm)	Dispersion (%)
Rh/Al_2O_3	0.09	0.022	20	54
Rh/CeO_2	0.04	0.049	30	47
Reactor				
0.32-cm-o.d. stainless-steel tubing				
Bed depth			1 cm	
Gas flow rate			50 cm^3/min (STP)	
Space velocity			82,000 h^{-1} (STP)	
Temperature			200–500°C	
Pressure			101.3 kPa (1 atm)	

widths were determined by scanning electron microprobe analysis.

The reactor was made of a 0.32-cm-o.d. stainless-steel tube packed with catalyst powder in the size range 80 to 120 mesh. The detailed characteristics of the catalyst and the reactor are listed in Table 1. The reactor temperature was measured in the middle of the bed and controlled electronically with a typical precision of ±1°C. The preheating of the feed gas was achieved in a blank alumina section located upstream of the reactor. The gas flow rate through the reactor was measured and controlled by electronic mass flow controllers. Transient responses of the gas-phase concentration in the exit stream from the reactor were monitored as a function of time by a mass spectrometer. The typical system response time from the reactor exit to the mass spectrometer was approximately 2 s. The pressure was reduced from atmospheric pressure at the reactor exit to 0.14 kPa at the sampling port of the mass spectrometer by a capillary tube. The pressure in the vacuum chamber of the mass spectrometer was maintained at approximately 10^{-6} kPa.

Initially the reactor was pretreated with 41 vol% H_2 in He flow (30 cc/min) for 5 h at 600°C to reduce the catalysts, followed by pretreatment with 4 vol% O_2 in He flow (30 cc/min) for 15 h at 600°C to oxidize the catalysts. Before each experimental run the reactor was pretreated with 30 cc/min flow of 0.16 vol% ^{13}CO in He for 30 min at 500°C in order to remove any oxygen accumulated on the catalyst surface during the previous experimental run. The reactor was then cooled down to a desired operating temperature in He flow, and the He flow was maintained for an additional 30 min to stabilize the reactor bed temperature. In the cycling experiments the pulse duration was controlled by a programmable timer. The transient response data were stored in an online computer and retrieved later for plotting on an X–Y recorder.

Since the reaction products CO_2 and N_2O have the same mass number of 44 under normal reaction conditions, a ^{13}CO isotope was used in place of CO so that $^{13}CO_2$ (mass number = 45) could easily be separated from N_2O. The purity of ^{13}C atoms in ^{13}CO was 99%. For simplicity in notation, CO will be used for ^{13}CO and CO_2 for $^{13}CO_2$ throughout the paper. A carbonyl trap packed with alumina pellets was placed in the CO flow line in order to avoid possible nickel (or iron) carbonyl contamination of catalysts. Standard cycling experiments involved introducing to the reactor an NO pulse of 30 s duration followed by a CO pulse of 30 s duration, as illustrated in Fig. 1. This process was repeated until the system was stabilized. In Fig. 1, τ is the cy-

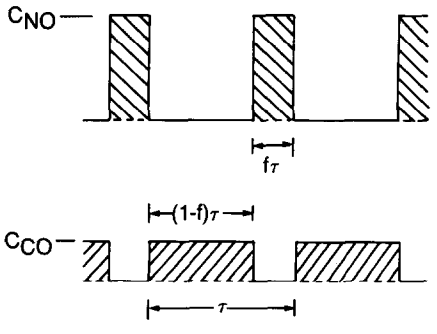

FIG. 1. The cycling scheme used for cyclic operation of the (CO + NO) reaction.

cling period and f denotes the duty fraction of NO feed during the cyclic operation such that

$$f = 0.5 \quad \text{and} \quad C_{CO} = C_{NO} \qquad (1)$$

for symmetric cyclic operation, and

$$f C_{NO} = (1 - f) C_{CO} \qquad (2)$$

for asymmetric cyclic operation. Thus, for both symmetric and asymmetric cyclic operations the time-average feed-stream concentrations of CO and NO were kept constant during each experimental run.

RESULTS

Symmetric Cycling Operation of (CO + NO) Reaction

In our earlier work (*20*) we observed that the NO decomposition activity of supported Rh catalysts decreases gradually as oxygen derived from NO decomposition accumulates on the catalysts. This suggests that the catalysts can be reactivated for NO decomposition by scavenging the oxygen using a reductant such as CO. In order to test the validity of this scheme for periodic deactivation/regeneration of catalysts, we performed a series of symmetric cycling operations with the Rh/Al_2O_3 catalyst under the conditions represented by Eq. (1) and Fig. 1. Note that the time-average concentration ratio of NO to CO in the feed was kept at unity in these experiments.

1. Effect of catalyst temperature. Presented in Figs. 2a through 2d are the effects of catalyst temperature on the transient behavior of the Rh/Al_2O_3 catalyst (as measured by the reactor outlet concentrations) during symmetric cycling operation with a cycling period of 60 s and $C_{CO} = C_{NO} = 800$ ppm. At room temperature (Fig. 2a) the Rh/Al_2O_3 catalyst exhibits virtually no activity for the (CO + NO) reaction. At 250°C (Fig. 2b) the catalyst exhibits relatively strong activity toward NO decomposition (as evidenced by N_2 formation) and CO oxidation (as evidenced by CO_2 formation): Note, however, that NO decomposes to nitrogen and oxygen only during the first 7 s of the NO half-cycle, and then the catalyst starts to lose its NO decomposition activity. The oxygen produced from the NO decomposition accumulates on the catalytic surface (as evidenced by the absence in the gas-phase responses of Fig. 2) and is reacted to form CO_2 during the subsequent CO half-cycle. For the CO half-cycle, CO_2 is produced for a short time until all available oxygen is consumed by CO and unreacted CO starts to appear in the effluent stream. Note that the time scale for regeneration during the CO half-cycle is comparable to that for deactivation during the NO half-cycle.

It is interesting to see two peaks associated with CO_2 formation: one at the beginning of the CO half-cycle and the other at the beginning of the NO half-cycle. The former is due to the oxygen stored during the previous NO half-cycle which reacts with CO during the CO half-cycle, while the latter is due to the adsorbed CO on the sur-

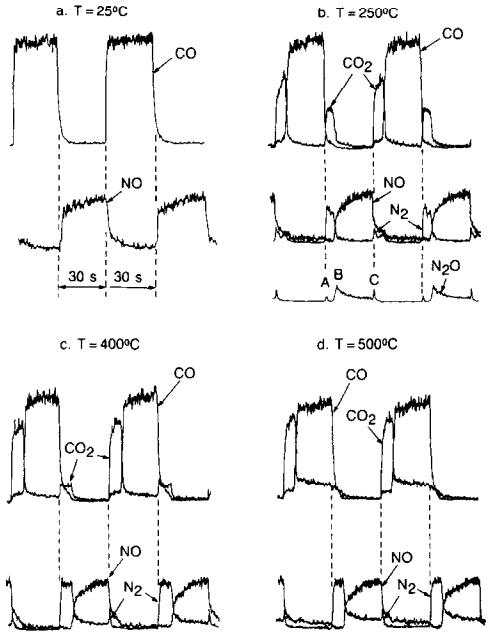

FIG. 2. Time variations of the reactor outlet concentrations at (a) 25°C, (b) 250°C, (c) 400°C, and (d) 500°C during symmetric cycling operation over Rh/Al_2O_3 ($\tau = 60$ s, $f = 0.5$, $C_{CO} = C_{NO} = 800$ ppm).

face which reacts with the oxygen being produced by NO decomposition during the NO half-cycle. Similarly, N_2 formation has two peaks: one at the start of the NO half-cycle and the other at the start of the CO half-cycle. The former is due to the decomposition of NO on the reduced Rh surface during the NO half-cycle, whereas the latter is mainly due to the adsorbed NO being decomposed to N_2 and oxygen as CO starts to reduce the oxidized Rh surface during the CO half-cycle. (A small fraction of this N_2 might be from the adsorbed nitrogen atoms being replaced by the incoming CO at the beginning of the subsequent CO half-cycle.) The significant amount of N_2O formation during the NO half-cycle in Fig. 2b (at 250°C) is in agreement with results reported previously (*20*). Among the three N_2O peaks observed in Fig. 2b (A, B, and C), one local maximum (A) is observed when the N_2 concentration is high but the NO concentration is low in the gas phase, whereas the other local maximum (C) occurs when the N_2 concentration is low but the NO concentration is high. The global maximum (B) occurs when both NO and N_2 concentrations are high. These observations are suggestive of the following N_2O formation mechanism on the surface in line with Chin and Bell (*24*), namely,

$$NO_a + N_a \rightarrow N_2O_a + S, \qquad (3)$$

where the subscript a denotes adsorbed state.

It should be noted that the CO_2 formation at the beginning of the NO half-cycle and the N_2 formation at the beginning of the CO half-cycle result from adsorbed CO and NO stored on the catalytic surface and that they contribute significantly to the overall extent of the (CO + NO) reaction during cyclic operation at low temperatures. A detailed discussion of such storage (or memory) effects of adsorbed reactants on time-average catalyst performance during cyclic operation can be found elsewhere (*25, 26*). At high temperatures, however, the storage effects of CO and NO become less important. At 400°C (Fig. 2c), for example, CO_2 and N_2 produced at the start of the NO and CO half-cycles, respectively, are considerably smaller than those at 250°C (Fig. 2b). This implies that the performance of cyclic operation can deteriorate as the catalyst temperature increases as will be shown later. At 500°C (Fig. 2d) the storage effect of adsorbed CO and NO disappears and the reaction products CO_2 and N_2 appear only at the beginning of the CO and NO half-cycles, respectively.

2. Effect of cycling period. The transient response of the Rh/Al_2O_3 catalyst during symmetric cycling was examined at a catalyst temperature of 500°C for three different cycling periods of 60, 20, and 10 s. The results for the cycling period of 60 s were already shown in Fig. 2d, where NO decomposition activity starts to decay at 7–8 s into the NO half-cycle with a time-average NO conversion of 50.8%. When the cycling period is reduced to 20 s (Fig. 3a), the NO decomposition activity starts to decay at 5–6 s into the NO half-cycle, yielding a time-average NO conversion of 76.5%. For the cycling period of 10 s (Fig. 3b) a nearly complete conversion of CO and NO was achieved with virtually no breakthrough of CO and NO. That is, the catalyst has an adequate capacity to store oxygen produced from NO decomposition for 5 s so that the catalyst deactivation can be avoided. Obviously, this observation has an important implication in the design and op-

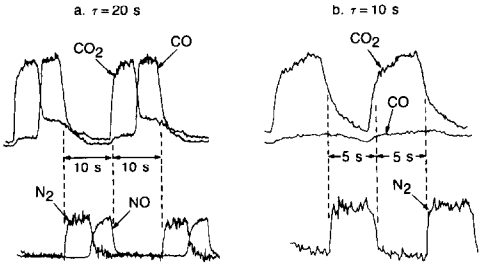

FIG. 3. Effect of cycling period on the transient response of Rh/Al_2O_3 during symmetric cycling ((a) τ = 20 s, (b) τ = 10 s, T = 500°C, $C_{CO} = C_{NO}$ = 800 ppm).

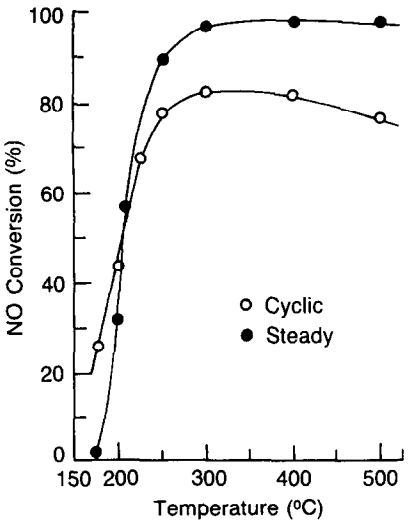

FIG. 4. Comparison between cyclic and steady performance of Rh/Al_2O_3 catalyst (τ = 20 s, symmetric cycling, $C_{CO} = C_{NO}$ = 800 ppm).

eration of closed-loop emission control systems, because it implies that, as far as the catalyst has an adequate oxygen storage capacity, the three-way catalyst need not be operated strictly at steady state in order to obtain adequate NO conversion performance.

Comparison between Cyclic and Steady Performance

The performance of the Rh/Al_2O_3 catalyst for the (CO + NO) reaction under cyclic operating conditions was compared with that under steady-state operating conditions at varying temperatures. The cycling scheme involved a symmetric cycling around the time-average reactant feed ratio of 1 with an amplitude of 800 ppm CO and NO in each of the CO and NO half-cycles, respectively. It is seen in Fig. 4 that reaction lightoff occurs at approximately 210°C. Above the reaction lightoff temperature steady operation yields better catalyst performance than cyclic operation, while the reverse is true below the reaction lightoff temperature. A similar trend has previously been observed during laboratory CO oxidation (*27*) as well as engine exhaust emission studies (*6*). It is remarkable that the general principle proposed earlier (*6*) regarding the cyclic performance of catalysts relative to the steady performance for binary surface reactions has been verified by yet another reaction system in this work. The negative slope in the cyclic performance curve in Fig. 4 at high temperatures above 300°C is physically related to the decreasing residence time (or decreasing storage effect) of adsorbed CO and NO on the surface as catalyst temperature increases as discussed earlier. A detailed discussion can be found elsewhere (*27*) on why the cyclic performance deteriorates at high temperatures while the steady performance does not.

Effect of Feed Composition on Steady-State Performance

For convenience in further discussions we express the stoichiometry of the feedstream in terms of the "stoichiometric number" (SN), defined as

$$\text{SN} = \frac{\text{time-average feed concentration of NO}}{\text{time-average feed concentration of CO}}$$

Note that SN = 1 corresponds to a stoichiometric feed composition for the reaction

$$NO + CO \rightarrow \tfrac{1}{2}N_2 + CO_2, \qquad (4)$$

while for the reaction

$$2NO + CO \rightarrow N_2O + CO_2 \qquad (5)$$

the stoichiometric feed composition corresponds to SN = 2. Even though reaction (5) involving N_2O formation has often been neglected in the literature for the analysis of steady-state (CO + NO) reaction data over Rh/Al_2O_3, we will consider the parallel reaction system described above [i.e., Eqs. (4) and (5)] in this study.

Figure 5 shows the NO conversion as a function of temperature for different values of the stoichiometric number during the steady-state (CO + NO) reaction over Rh/

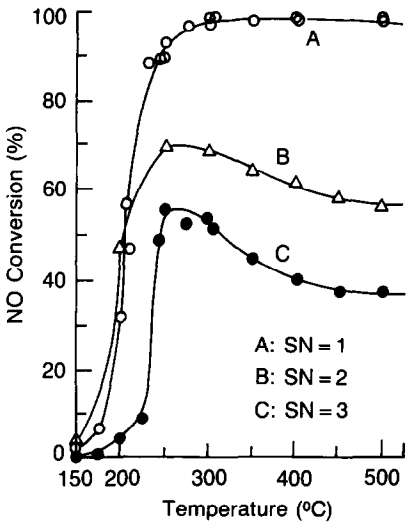

FIG. 5. Effect of feed composition on steady-state performance of Rh/Al_2O_3 for the (CO + NO) reaction.

Al_2O_3. The stoichiometric number was varied by changing the feed concentration of CO while keeping the feed concentration of NO constant at 400 ppm. Interestingly there exists a maximum in NO conversion for all SN values of 1, 2, and 3. Although the presence of a maximum is not pronounced for SN = 1 (curve A), the decreases in NO conversion at high temperatures for SN = 2 and 3 (curves B and C) are rather dramatic. More interesting is that the NO conversions for curves B and C cannot be explained by reaction (4) alone; that is, if reaction (4) were the only pathway for removing NO, the NO conversions for SN = 2 and 3 would not exceed 50 and 33%, respectively. This contradicts the results shown in Fig. 5 and immediately suggests a significant contribution of reaction (5) to the overall conversion of NO.

Figure 6 illustrates the impact of the N_2O formation on the overall conversion of NO for SN = 1. The symbols δ_{NO} and δ_{CO} refer to the amounts of NO and CO consumed during the steady-state operation of the (CO + NO) reaction, respectively. The discrepancies between δ_{NO} and δ_{CO} observed over the entire temperature range are not consistent with reaction (4). The difference between δ_{NO} and δ_{CO} can be correlated very well with the amount of N_2O formation (δ_{N_2O}) as shown in Fig. 6b. We note that the temperature for maximum N_2O formation in Fig. 6b corresponds to the reaction lightoff temperature in Fig. 6a, suggesting that the N_2O formation according to reaction (5) may play an important role in initiating the (CO + NO) reaction.

The maximum in the NO conversion with increasing temperature (see Fig. 5) for SN greater than 1 can also be explained on the basis of the N_2O formation. Figure 7a shows δ_{NO} and δ_{CO} plotted as a function of temperature for SN = 3. While δ_{NO} has a maximum at 275°C, δ_{CO} increases monotonically with increasing temperature. Furthermore, δ_{CO} remains essentially constant above 250°C. Again this is not consistent with reaction (4), which requires that δ_{NO} and δ_{CO} be the same at all temperatures.

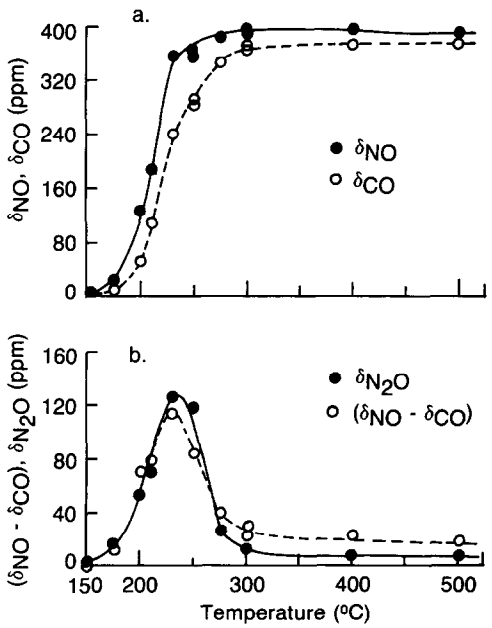

FIG. 6. Amounts of NO and CO disappeared and their relation to the amount of N_2O formed during steady-state (CO + NO) reaction (SN = 1).

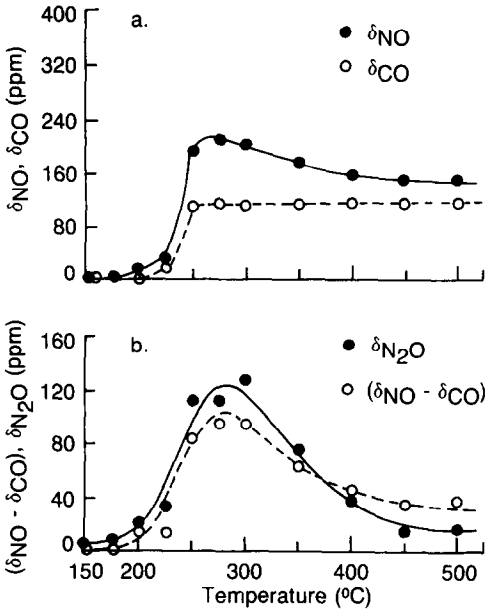

FIG. 7. Amounts of NO and CO disappeared and their relation to the amount of N_2O formed during steady-state (CO + NO) reaction (SN = 3).

Instead, the difference between δ_{NO} and δ_{CO} can be reasonably well correlated with δ_{N_2O} as shown in Fig. 7b. Comparison of Fig. 7a with 7b reveals that similar temperatures are required for the onset of both the N_2O formation and the (CO + NO) reaction.

In order to examine the importance of reaction (5) relative to reaction (4), the ratio of N_2O (C_{N_2O}) to N_2 (C_{N_2}) produced during the steady-state (CO + NO) reaction over Rh/Al_2O_3 is plotted in Fig. 8 as a function of catalyst temperature for SN = 1 and 3. We want to point out two observations in Fig. 8. First, the N_2O formation becomes more important as the catalyst temperature decreases, especially below the reaction lightoff temperatures. Second, at a given temperature the relative importance of the N_2O formation increases as the stoichiometric number increases (i.e., as the gas-phase composition becomes more oxidizing condition). Thus, for SN = 3 the N_2O formation is not negligible even at 500°C.

On the basis of the above observations we are led to the following conclusions:

(i) The N_2O formation reaction (5) plays an important role when the catalyst temperature is low and/or NO concentration is high relative to CO concentration.

(ii) The maximum in a plot of NO conversion vs temperature during the steady-state (CO + NO) reaction correlates well with the N_2O formation via reaction (5).

It seems reasonable to propose that below the reaction lightoff temperature the oxygen produced during the NO reduction via

$$2NO_a \rightarrow N_2O_a + O_a \qquad (6)$$

helps initiate the surface reaction between CO_a and O_a. This may provide an explanation for the observations of Figs. 6a and 7a that NO conversion precedes CO conversion.

Effect of Time-Average Feed Composition on Cyclic Performance

The effects of the time-average feed composition on NO conversion during symmetric cycling operation of the (CO + NO) re-

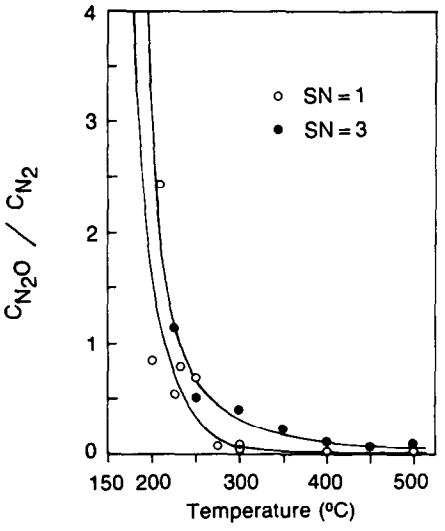

FIG. 8. Effect of catalyst temperature on the ratio of N_2O to N_2 formed during steady-state (CO + NO) reaction over Rh/Al_2O_3.

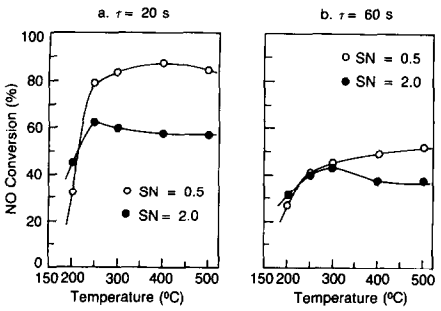

FIG. 9. Effect of time-average feed composition on cyclic performance of Rh/Al_2O_3 ((a) τ = 20 s, (b) τ = 60 s).

action over Rh/Al_2O_3 were examined by varying the concentration of the CO pulse while keeping the concentration of the NO pulse constant at 800 ppm. The results are shown in Figs. 9a and 9b for cycling periods of 20 and 60 s, respectively. In both cases, reaction lightoff occurs around 225°C. Note, however, that sharper reaction lightoff was observed for fast cycling than for slow cycling. Below the reaction lightoff temperature an increase in CO concentration (i.e., decrease in SN) impairs the cyclic performance, while above the reaction lightoff temperature it improves the cyclic performance. The high-temperature behavior is consistent with the inhibition effect of strongly adsorbed oxygen on NO decomposition (*20*), while the low-temperature behavior is consistent with the inhibition effect of strongly adsorbed CO on the CO oxidation (*12*).

Comparison of Fig. 9a with 9b shows that the shorter cycling period (20 s) yields better performance than the longer cycling period (60 s). As the cycling period increases, the effect of stoichiometric number in the feed stream becomes less significant. This is due to the nature of the life cycle of this process. That is, for sufficiently long cycling periods, the effect of SN should essentially disappear because the NO decomposition activity (and thus the NO conversion performance) would be limited by the oxygen storage capacity of the catalyst.

Effect of Oxygen Storage Capacity of Support

In the previous section we have shown that regeneration of Rh/Al_2O_3 catalysts for the (CO + NO) reaction under cycled operating conditions involves the removal of surface oxygen through reaction with the reductant CO. Thus, increasing the CO concentration in the feed enhances the NO reduction activity at high temperatures, owing to the increased oxygen scavenging activity by CO, as shown in Fig. 9. Another way of improving the NO decomposition activity over Rh would be to increase the oxygen storage capacity of the catalyst by employing CeO_2 (in place of Al_2O_3) as the catalyst support (*20*); ceria has been widely used as an additive in three-way catalysts to promote the water–gas shift reaction as well as to store and release oxygen during cyclic operation of three-way catalytic converters (*28–30*). This idea has prompted us to test the CeO_2 support as an oxygen storage component during the cycling operation.

Recall that the NO conversion activity of the Rh/Al_2O_3 catalyst at 500°C under symmetric cycling conditions with a cycling period of 20 s started to decay at about 5 s into the NO half-cycle with a time-average NO conversion of 76.5% (see Fig. 3). Figure 10 shows the cyclic performance of the Rh/CeO_2 catalyst under the same operating conditions as those in Fig. 3a. Here the deactivation of the Rh/CeO_2 catalyst for NO decomposition occurs at about 7 s into the NO half-cycle, which is a substantial improvement over the Rh/Al_2O_3 catalyst. This is consistent with the previous observations that the lifetime of noble metal catalysts for NO decomposition can be extended by using CeO_2 in place of Al_2O_3 support (*20*). The resulting improvement in NO conversion along with corresponding CO_2 production is remarkable; the time-average NO conversion was observed to be 93.6%. This conversion enhancement can be attributed to the large oxygen storage capacity of CeO_2

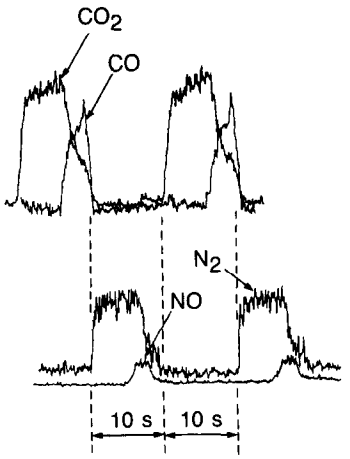

FIG. 10. Cyclic performance of Rh/CeO_2 catalyst (T = 500°C, τ = 20 s, f = 0.5, $C_{CO} = C_{NO}$ = 800 ppm).

compared with that of Al_2O_3 (*20*). Further results on the catalytic activity of the Rh/CeO_2 catalyst for the (CO + NO) reaction during cyclic operation will be reported in a forthcoming paper.

Effect of Asymmetric Cycling

In our earlier discussions regarding symmetric cycling operation, we came to the conclusion that the nature of the rate-controlling step changes with temperature; below reaction lightoff temperature the oxygen-producing mechanism via NO decomposition is the rate-controlling step, while above the reaction lightoff temperature the oxygen-scavenging mechanism via CO oxidation is the rate-controlling step. Now one obvious question is whether cyclic performance can be further improved by employing an asymmetric cycling strategy instead of a symmetric cycling. For example, Taylor and Sinkevitch (*31*) observed that under certain conditions asymmetrically cycling the feed composition gives higher conversion than does symmetric cycling in their laboratory experiments using an exhaust-aged three-way catalyst. In this work we want to focus on the effect of varying the duty fraction of each half-cycle while keeping the time-average feed composition constant [according to Eq. (2)] during the cyclic operation. If the process is controlled by CO oxidation, the gas-phase CO concentration may be reduced with correspondingly increased duty fraction to keep the time-average feed composition constant. This mode of operation would reduce the competition for active catalytic sites among CO molecules in the gas phase, possibly resulting in an enhanced cyclic performance. Note that the extreme case is to feed CO to the reactor one molecule after another in order to ensure that every CO molecule consume one oxygen atom stored in the catalyst. Similarly, when the process is controlled by NO decomposition, the cyclic performance may be improved by reducing the gas-phase NO concentration with correspondingly increased duty fraction of the NO pulse.

The above idea has been tested experimentally, and the results are presented in Fig. 11. Details of the three different modes of cycling considered are listed in Table 2. (Note in Table 2 that the cycling mode B is

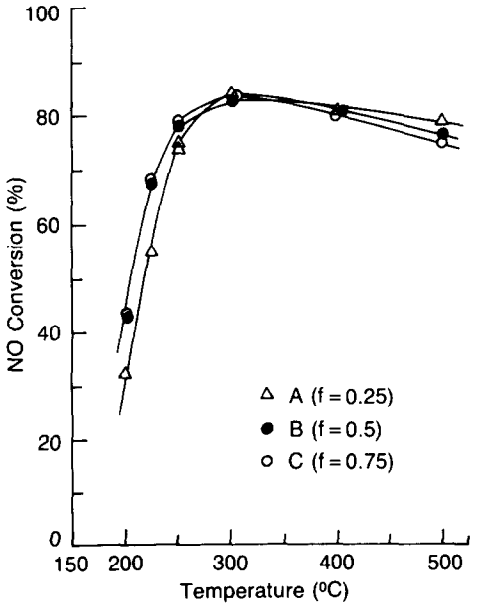

FIG. 11. Effect of asymmetric cycling on the performance of Rh/Al_2O_3 catalyst.

TABLE 2

Various Modes of Cycling Operation

	τ (s)	f	C_{NO} (ppm)	C_{CO} (ppm)
A (asymmetric)	20	0.25	800	267
B (symmetric)	20	0.5	800	800
C (asymmetric)	20	0.75	800	2400

symmetric cycling.) The time-average value of the stoichiometric number is 1 for all three cases. The asymmetric cycling mode C involves high CO concentration combined with low NO concentration, while the asymmetric cycling mode A is representative of low CO concentration combined with high NO concentration. Results shown in Fig. 11 indicate that at high temperatures (above 275°C) asymmetric cycling with low concentration and long duty fraction of CO pulse (cycling mode A) is preferable. At low temperatures (below 275°C), however, higher NO conversions were observed with cycling mode C. This behavior is in line with our expectations, considering the change in the rate-controlling processes with temperature as discussed earlier. It is probably fair to point out here that the effects of asymmetric cycling are rather minor in Fig. 11.

DISCUSSION

The feed composition cycling combined with steady-state kinetic measurements using an isotopic reactant (^{13}CO) has revealed interesting dynamic behavior of the (CO + NO) reaction over Rh/Al_2O_3. The formation of N_2O observed in this work is in line with those observed by Ilzuka and Lunsford (*32*), Hecker and Bell (*18, 19*), and Hyde *et al.* (*33*). Regarding the further reduction of N_2O by CO, Hecker and Bell (*18*) reported no measurable activity over Rh/SiO_2. However, we observed in a separate experiment good activity of Rh/Al_2O_3 for the (N_2O + CO) reaction under steady-state operating conditions as shown in Fig. 12. We have thus demonstrated, for the first time, the importance of the formation of N_2O as an *intermediate step* during the reduction of NO by CO over Rh/Al_2O_3. Now it appears reasonable to include the formation of adsorbed N_2O [see Eq. (3)] in the mechanism of the (CO + NO) reaction over Rh/Al_2O_3.

It is also noteworthy that Hyde *et al.* (*33*) proposed N_2O production from dinitrosyl species, $Rh(NO)_2$, present on individual Rh atom sites or edge sites with cationic character generated through interactions between metal atoms and alumina support. They also found that Rh/Al_2O_3 was rapidly poisoned as the N_2O production proceeded because the reactive sites were simultaneously poisoned by oxygen adatoms which prevented further decomposition of NO as a result of its competition for electronic charge from a chemisorbed NO molecule. The oxygen produced from NO decomposition was not readily desorbed from Rh below 550°C, which agrees with our results. It is also worth noting the molecular orbital calculations by Casewit and Rappé (*34*) who point out that the formation of dinitrosyl complex must be an intermedi-

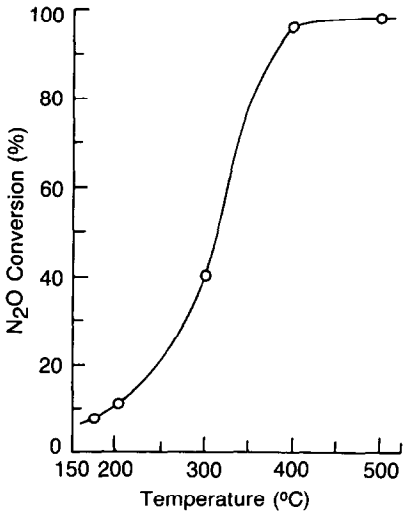

FIG. 12. Performance of Rh/Al_2O_3 catalyst for the (N_2O + CO) reaction under steady-state operating conditions ($C_{CO} = C_{N_2O} = 600$ ppm).

ate step in the formation of N_2O from NO on Fe(II) catalysts. On single-crystal Rh surfaces it is rather well established that the N–N bond forms between two N atoms derived from NO decomposition (*11, 16, 17*). On supported Rh catalysts, however, the formation of the N–N bond through the dinitrosyl complex may also be important in view of the previous observations on Fe catalysts (*14, 15, 34*).

On the basis our observations we propose the following overall reaction scheme for NO reduction by CO over Rh/Al_2O_3:

$$NO + CO \rightarrow \tfrac{1}{2}N_2 + CO_2 \quad (7)$$

$$2NO + CO \rightarrow N_2O + CO_2 \quad (8)$$

$$N_2O + CO \rightarrow N_2 + CO_2 \quad (9)$$

Note that we rewrote reactions (4) and (5) in reactions (7) and (8) above for the convenience of our discussion. Reactions (8) and (9) are important at low temperatures, while reaction (7) becomes important at high temperatures. As a result, the stoichiometric composition at low temperatures corresponds to the SN numbers ranging between 1 and 2 depending upon the reaction selectivity, while the stoichiometric composition at high temperatures is characterized by SN $\cong$ 1. It seems reasonable at this point to conclude that the formation and reduction of N_2O are important reaction steps in the mechanism of the (CO + NO) reaction over supported Rh catalysts, which is in line with the previous observations over transition metal oxides (*13*).

It should be noted that reaction (7) cannot be excluded from the list of reactions, even though it is a linear combination of reactions (8) and (9). The reason can be clearly seen by examining a detailed reaction mechanism based on the following sequence of elementary surface processes:

$$NO + S \leftrightarrows NO_a \quad (10)$$

$$CO + S \leftrightarrows CO_a \quad (11)$$

$$NO_a + S \rightarrow N_a + O_a \quad (12)$$

$$NO_a + N_a \rightarrow N_2O_a + S \quad (13)$$

$$N_2O_a \leftrightarrows N_2O + S \quad (14)$$

$$N_2O_a \rightarrow N_2 + O_a \quad (15)$$

$$N_a + N_a \rightarrow N_2 + 2S \quad (16)$$

$$CO_a + O_a \rightarrow CO_2 + 2S \quad (17)$$

The elementary surface processes (10), (11), (12), and (17) are the same as those proposed by Hecker and Bell (*19*) who excluded from their mechanism the formation [step (13)] and decomposition [step (15)] of N_2O_a as well as the reduction of N_2O_a by CO_a [steps (15) and (17)]. The adsorbed state of N_2O in our proposed mechanism above is consistent with the literature (*35*) where N_2O_a was observed on Rh/Al_2O_3 at 2245 cm^{-1} of infrared adsorption band. The mechanism of the decomposition of N_2O_a [step (15)] to produce O_a is supported by our observation (see Fig. 12) in the (N_2O + CO) reaction which produced N_2 and CO_2. Note that the combination of steps (12) and (13) reduces to the mechanism (6) proposed earlier and that the combination of steps (13) and (14) reduces to the N_2O formation mechanism proposed by Hecker and Bell (*18, 19*). Note also that reaction (7) involves elementary surface processes (10), (11), (12), (16), and (17); reaction (8) involves (10), (11), (12), (13), (14), and (17); reaction (9) involves (14), (15), and (17).

We have shown that there is a temperature where the steady-state kinetics of the (CO + NO) reaction has a maximum NO conversion, which cannot be explained by the corresponding CO conversion. We have demonstrated that this maximum in the NO conversion can be attributed to the reduction of NO to N_2O according to reaction (8). For the (CO + NO + O_2) reaction over Rh/Al_2O_3 and Ir/Al_2O_3 catalysts, Taylor and Schlatter (*10*) observed similar maxima in NO conversions which they could not explain in terms of the corresponding CO conversions. Even though their reaction system (CO + NO + O_2) is different from ours, it is reasonable to believe that the N_2O for-

mation mechanism was partially, if not totally, responsible for the maxima in the NO conversions.

At low temperatures the (CO + NO) reaction is controlled by the oxygen generating process through the decomposition of NO, while at high temperatures the (CO + NO) reaction is controlled by the oxygen-scavenging process through a reaction between CO_a and O_a. This oxygen-scavenging process as a rate-controlling step at high temperatures suggests another means of oxygen scavenging during cyclic operation: that is, the use of an oxygen storage component, CeO_2, as catalyst support. The validity of this idea was clearly demonstrated by the enhanced catalytic activity of the ceria-supported Rh catalyst compared with the alumina-supported counterpart.

In our earlier work we proposed a general principle for the enhancement of catalytic activity by cyclic operation: below reaction lightoff temperature cyclic operation performs better than steady operation, while above the reaction lightoff temperature the cyclic operation deteriorates catalyst performance (*6, 27*). This work provides another sample for which this principle holds.

During the last decade there has been much discussion on the formation of isocyanate species (NCO) during the (CO + NO) reaction over supported Rh catalysts [e.g., (*19, 35, 36*)]. However, studies of the formation and decomposition of the Rh–NCO (*19, 35*) suggest that the NCO species present on RH is not directly involved in the formation of the reaction products observed in this study. Thus, this species appears to have no direct effect on the kinetics of the (CO + NO) reaction and thus should have no effect on the interpretation of our results.

SUMMARY AND CONCLUSIONS

The catalytic activity of Al_2O_3- and CeO_2-supported Rh catalysts for the reduction of NO by CO under cycled and steady feedstream conditions was investigated using a packed-bed reactor and an isotopic reactant, ^{13}CO. The major findings of this study are listed below.

1. We have identified the formation of N_2O as an important *intermediate step* during the (CO + NO) reaction over Rh/Al_2O_3. Accordingly we propose that the following three reactions are involved for the reduction of NO by CO:

$$CO + NO \rightarrow \tfrac{1}{2}N_2 + CO_2$$

$$CO + 2NO \rightarrow N_2O + CO_2$$

$$CO + N_2O \rightarrow N_2 + CO_2$$

2. When the NO/CO ratio is greater than 1, the NO conversion during the steady-state (CO + NO) reaction has a maximum as a function of temperature. This observation can be explained on the basis of the temperature dependence of the N_2O formation rate.

3. Below reaction lightoff temperature the rate of the (CO + NO) reaction is controlled by the rate of oxygen production via NO decomposition, while above the reaction lightoff temperature it is controlled by the rate of oxygen scavenging from the surface via CO oxidation.

4. Below the reaction lightoff temperature, cyclic operation performs better than steady operation, whereas this trend reverses above the reaction lightoff temperature. This result confirms the validity of the hybrid feed composition control scheme proposed earlier for improved operation of catalysts (*6, 27*).

5. Ceria support improves the catalyst performance significantly compared with alumina support during cyclic operation at 500°C. This enhanced catalytic activity can be attributed to the ability of the ceria support to store a greater amount of oxygen during the cyclic operation.

ACKNOWLEDGMENT

The catalysts were prepared by C. J. Stock.

APPENDIX: NOMENCLATURE

C_{CO} feed concentration of CO (mol/cm^3)
C_{NO} feed concentration of NO (mol/cm^3)
C_{N_2O} feed concentration of N_2O (mole/cm^3)
f duty fraction of NO pulse during cyclic operation
S active surface sites (mol/cm^2)
δ_{CO} amount of CO disappeared in (CO + NO) reaction (ppm)
δ_{NO} amount of NO disappeared in (CO + NO) reaction (ppm)
δ_{N_2O} amount of N_2O formed in (CO + NO) reaction (ppm)
τ cycling periods (s)

Subscripts

a adsorbed state

REFERENCES

1. Kummer, J. T., *Prog. Energy Combust. Sci.* **6,** 177 (1980).
2. Taylor, K. C., *in* "Catalysis: Science and Technology" (J. R. Anderson, and M. Boudart, Eds.), Vol. 5. Springer-Verlag, Berlin, 1984.
3. Adams, K. M., and Gandhi, H. S., *Ind. Eng. Chem. Prod. Res. Dev.* **22,** 207 (1983).
4. Yokoda, K., Muraki, H., and Fujitani, Y., SAE Paper 850129, 1985.
5. Muraki, H., Shinjoh, H., and Fujitani, Y., *Appl. Catal.* **22,** 325 (1986).
6. Cho, B. K., *Ind. Eng. Chem. Res.* **27,** 30 (1988).
7. Kobylinski, T. P., and Taylor, B. W., *J. Catal.* **33,** 376 (1974).
8. Arai, H., and Tominaga, H., *J. Catal.* **43,** 131 (1976).
9. Campbell, C. T., and White, J. M., *Appl. Surf. Sci.* **1,** 347 (1978).
10. Taylor, K. C., and Schlatter, J. C., *J. Catal.* **63,** 53 (1980).
11. Root, T. W., Schmidt, L. D., and Fisher, G. B., *Surf. Sci.* **150,** 173 (1985).
12. Oh, S. H., Fisher, G. B., Carpenter, J. E., and Goodman, D. W., *J. Catal.* **100,** 360 (1986).
13. Shelef, M., and Otto, K., *J. Catal.* **10,** 408 (1968).
14. Fu, C. M., Korchak, V. N., and Hall, W. K., *J. Catal.* **68,** 166 (1981).
15. Petunchi, J. O., and Hall, W. K., *J. Catal.* **78,** 327 (1982).
16. Root, T. W., Schmidt, L. D., and Fisher, G. B., *Surf. Sci.* **134,** 30 (1983).
17. Castner, D. G., and Somorjai, G. A., *Surf. Sci.* **83,** 60 (1979).
18. Hecker, W. C., and Bell, A. T., *J. Catal.* **84,** 200 (1983).
19. Hecker, W. C., and Bell, A. T., *J. Catal.* **85,** 389 (1984).
20. Cho, B. K., and Stock, C. J., presented at the 1986 Annual Meeting of American Institute of Chemical Engineers, Miami Beach, FL, November 1986.
21. Weekman, V. W., *Inc. Eng. Chem. Proc. Des. Dev.* **7,** 252 (1968).
22. Monroe, D. R., and Leiferman, M. W., General Motors Research Laboratories, Warren, MI, private communications, 1987.
23. D'Aniello, M. J., U.S. Patent 4,380,510 (1983).
24. Chin, A. A., and Bell, A. T., *J. Phys. Chem.* **87,** 3700 (1983).
25. Cho, B. K., *Ind. Eng. Chem. Fundam.* **22,** 410 (1983).
26. Herz, R. K., Kiela, J. B., and Sell, J. A., *Ind. Eng. Chem. Prod. Res. Dev.* **22,** 387 (1983).
27. Cho, B. K., and West, L. A., *Ind. Eng. Chem. Fundam.* **25,** 158 (1986).
28. Summers, J. C., and Ausen, S. A., *J. Catal.* **58,** 131 (1979).
29. Schlatter, J. C., and Mitchell, P. J., *Ind. Eng. Chem. Prod. Res. Dev.* **19,** 288 (1980).
30. Herz, R. K., *Ind. Eng. Chem. Prod. Res. Dev.* **20,** 451 (1981).
31. Taylor, K. C., and Sinkevitch, R. M., *Ind. Eng. Chem. Prod. Res. Dev.* **22,** 45 (1983).
32. Ilzuka, T., and Lunsford, J. H., *J. Mol. Catal.* **8,** 391 (1980).
33. Hyde, E. A., Rudham, R., and Rochester, C. H., *J. Chem. Soc. Faraday Trans. 1* **80,** 531 (1984).
34. Casewit, C. J., and Rappé, A. K., *J. Catal.* **89,** 250 (1984).
35. Solymosi, F., and Sarkany, J., *Appl. Surf. Sci.* **3,** 68 (1979).
36. Kiss, J., and Solymosi, F., *Surf. Sci.* **135,** 243 (1983).